

DETC99/VIB-8323

AERODYNAMIC FLOW CONTROL USING SHAPE ADAPTIVE SURFACES

N. J. Pern* and J. D. Jacob†
Department of Mechanical Engineering
University of Kentucky
Lexington, KY 40506-0108
E-mail: jdjacob@uky.edu

ABSTRACT

The present paper discusses results of experiments on flow control using an adaptive circular arc airfoil. A modified THUNDER actuator (piezoceramic bonded with a metallic substrate) serves as an adaptive airfoil that allows leading edge displacements of approximately 1 cm. The airfoil's radius of curvature R_c is varied by altering the voltage applied across the upper and lower surfaces. The maximum input voltage varies $R_c \pm 2\%$ resulting in a variation in the lift coefficient C_l of approximately 7% at a frequency up to 25 Hz. Results of wake mitigation and flutter control tests are briefly discussed.

INTRODUCTION

Flow control, particularly active flow control, represents the sine qua non of applied fluid dynamics. As a general design tool, flow control is not yet a mature technology but the lure of its many practical uses makes it a much researched area of flow engineering (e.g., see Wygnanski (1)). Much of the research in active flow control has focused on using blowing and/or suction or MEMS devices attempt to essentially alter the boundary layer on the surface to control the flow. In essence, the devices actively alter the flow so that it adapts to the geometry. One may take the opposite approach, however, where the surface geometry actively adapts to changing flow conditions. This is the case we are interested in here.

Adaptive wings, i.e., wings whose shape can be altered in flight, have the promise of revolutionizing aeronautics (e.g., (2)).

Recent research has been conducted into adaptive airfoils from both theoretical and engineering standpoints. While the benefits of an airfoil whose geometry is variable in flight is readily seen, the current state-of-the-art lacks the stringent requirements for practical application. This is exacerbated since the complexity of the problem often calls for examinations of potential adaptive systems from a single perspective rather than considering the physics of the whole system; viz., aerodynamics, structural dynamics, and control. This includes work such as the development of flexible airfoils whose thinness precludes structural development with current materials or wings with bulky and heavy actuation systems which negate the benefit of the adaptive design. However, recent developments have shown that a viable adaptive wing is in the foreseeable future.

The primary motive for altering wing geometry is to improve airfoil efficiency in off-design flight regimes. This concept is a standard implementation in most modern aircraft designs and takes the form of flaps which change the wing area and/or effective camber. A polymorph wing (variable planform) and variable pitch or incidence are also proven methods of wing adaptation. Adaptive concepts have taken many forms and names, including deformable, flexible, and active, in addition to those previously mentioned. In this paper, however, we will use the term *adaptive* to indicate an airfoil whose actual (as compared to effective) profile can be altered during flight.

The ideal use of an adaptive strategy allows the wing to vary its geometric parameters in flight during encounters in situ of changing flow conditions such as wind speed or direction. As much of the governing principles of the unsteady fluid/structure interactions are unknown, extensive research into the physics is

*Graduate student; member ASME.

†Assistant Professor; member ASME.

necessary, including the dynamics of series adaptive paneling, the actuation and control of an adaptive wing in flight, and real-time unsteady aerodynamic measurement and analysis. It is the dynamics of the fluid/structure interface that interest us here, primarily the aeroelastic transient coupling of the varying airfoil parameters and the unsteady flow. As the wing changes geometry, the flow will rapidly follow these changes. However, since the flow is a continually evolving structure, the altered flow field can interact with the wing in a nonlinear fashion. To determine the desired singular or periodic variations in wing geometry a priori, it will be necessary to first understand the underlying physics. The number of variables results in an inordinately large parameter space which suggests the use of simulations should be used in tandem with any experimental investigation.

Range of Interest

The qualitative aerodynamic characteristics of low Re flows are typically vastly different than those normally seen in typical aerodynamic and aerospace applications (3; 4). Slight changes in the flow speed can have large effects on the flow over a given airfoil, most notably severe changes in L/D ratio. The wing shape can be specifically tailored for a certain Re , but designing for a larger range of Re will degrade performance for a specific wing velocity. Two classes of aircraft fly in the low to moderate Re range: Micro Aerial Vehicles (μ AVs) and Unmanned Aerial Vehicles (UAVs or RPVs). In the former case, Re may range from $10^4 - 10^5$ and lower if hovering/loitering vehicles are considered. In the latter case, Re typically increases from 10^5 upwards to 10^6 and higher for the larger faster aircraft. Due to the nature of these vehicles, the technology described herein is well suited for μ AV and UAV application inasmuch as the Re range of these vehicles allows the flow to be easily adjusted using wing shaping (16).

Sub-scale air vehicles such as μ AVs and UAVs often have the disadvantage of lower lift capabilities due to reduced size but increased weight penalties due to a minimum size of control surfaces. The primary advantage of a μ AV is its small size allowing it to go unnoticed on the battlefield. It is ideally suited for covert operations where surprise and advanced intelligence are key components of a successful mission. The size limit of μ AVs are typically given as less than 15 cm in maximum length (5; 16). For a standard wing planform, this gives a span of $b = 15$ cm. If a moderate aspect ratio of 4 is assumed and the vehicle is to move at a relatively slow speed, say 10 m/s, an estimate for even high lift coefficients results in lift forces on the order of 0.5 N (0.1 lbs.) or less. This weight leaves little room for equipment, let alone the vehicle structure and powerplant itself. And if the vehicle were to encounter a gust in the same direction as flight, the vehicle would probably crash. Since μ AVs are still in the early development stages, issues such as operation, safety, reliability, robustness, affordability, packaging and other operational factors cannot be adequately discussed.

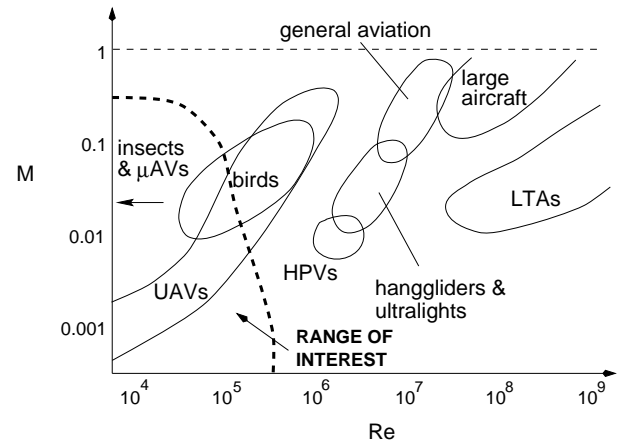


Figure 1. Range of interest on the Re - M diagram.

As an option to μ AV utilization, an adaptive wing can be installed on a UAV/RPV. This has many of the same characteristics of a μ AV, only on a larger scale. UAVs are typically designed for a single mission in mind, usually long-range cruise. For UAVs which have varied mission goals, however, such as loiter, encounter, and then rapid return, the vehicle may experience a variety of flight regimes. An adaptive wing would be an ideal lifting system for such a vehicle. While it would be possible to retrofit an existing UAV with an adaptive wing, it would probably be more cost efficient to design a new UAV around an adaptive wing system.

Adaptive Wing Developments

One of the early departures from the philosophy which treated aircraft wings as rigid structures discussed the advantages of structural tailoring in aircraft (6). This approach takes advantage of characteristics such as structural anisotropy and elastic coupling to enhance a particular structural response. This approach to airfoil design has been demonstrated to yield significant benefits. It provided the framework for subsequent investigations that added active elements to improve upon the already significant benefits of structural tailoring. Further studies examined in detail the interaction between aerodynamic forces, structural forces, conventional control forces, and an additional control force arising from inclusion of active materials in the wing structure (7). A mathematical foundation was presented that argued that the inclusion of active materials in the wing structure could be used to advantage to increase wing speed divergence, reduce gust loading, and change lift effectiveness. It is clear that an ability to control these wing characteristics in a practical fashion would lead to a wing design which is beneficial to aircraft performance.

Active elements were added later to enhance structural tailor-

ing effects (8). This work was a largely experimental study where the static shape of a prototype F-14 wing cross-section was controlled with an array of linear actuators that acted as both wing spars and actuators to control wing shape. The stated goal of this study was the reduction of shock-induced drag in transonic cruise and multi-DOF shape control was demonstrated that could potentially address this problem.

Modeling of aeroelastic structural tailoring and adaptive wings (those that incorporate active materials) were more fully examined using a thick walled composite beam representative of the structure of a modern aircraft wing (9). The wing model included anisotropy and coupling to allow structural tailoring and active layers to provide shape control. The results of this extensive modeling effort indicated that the combination of structural tailoring and adaptive wing shape control can improve the vibrational and static aeroelastic response of aircraft wings.

The papers mentioned above represent an overview of the early work in adaptive wing modeling. This area has matured to the point where significant experimental verification work is now taking place. Recent tests of a piezoelectric actuator driven adaptive wing were used to demonstrate active flutter control (10). Also discussed were tests investigating alleviation of vertical tail buffeting and wing shape control using piezoelectric actuators applied to load-bearing structural members. Development of wind tunnel models and results of wind tunnel tests of adaptive wing models have also been demonstrated (11; 12; 13). Both investigations lend credence to the basic concept of the adaptive wing as a practical design option for an aircraft wing. An adaptive airfoil design designated the Dynamically Deforming Leading Edge (DDLE) airfoil varies the leading edge radius in flight by stretching its thin composite skin (14). The primary objective for this development is to achieve effective flow control over the airfoil through the reduction of strong adverse pressure gradient that leads to wing stall. Recent investigations into flexible wing architectures have shown the possibility of their use in adaptive wing technology as well (15; 16).

Smart Materials

Conventional means of wing shaping require in-wing actuators and additional lifting surfaces. These are typically rigid attachments to the main wing and the profile is altered to an equivalent profile by gross adjustments. These are typically only good in a small range of Re and M . To alter the wing profile in situ, internal actuators can be used to adjust such parameters as camber and thickness, but the adjustments are typically small and the actuators heavy. Thus, the benefits of wing shaping were outweighed by its added weight penalties.

Smart materials offer a more cost-feasible solution to this problem. The most common of smart material actuators are made of piezoelectric materials such as zinc oxide or lead zirconate titanate. These are based upon the piezoelectric effect where a

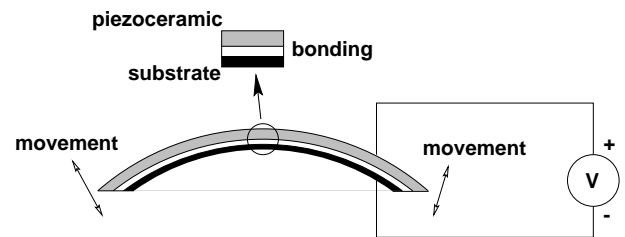


Figure 2. Piezoelectric THUNDER actuator.

A portion of an adaptive actuator using piezoelectric material. This specific design offers a good balance between force and deflection.

force is generated by a piezoelectric material when a differential voltage is applied. These have to be made relatively thick to prevent dielectric breakdown. Piezoelectric actuators can take many forms such as stacks or bimorphs. Both have been used with success in the construction of flaps for airfoils (17). These can be used alone or in conjunction with traditional systems, such as hydraulic or mechanical actuators. Piezoelectric actuators have been used by Clement et al. (18) for use in helicopter blade flaps. Other smart materials used in airfoil applications include shape memory alloys (SMA) such as Nitinol. These are metals that change shape when the temperature of the material changes. This can be accomplished by electrical current heating or Joule heating and then allowing the system to cool. Upon cooling, the material returns to its previous unheated shape. This system is particularly suited for use in hydrofoils where cooling is rapid (19). While the same precise control is typically not comparable to a MEMS device, the cost-savings benefits are worth the small reduction in performance.

In essence, control of the adaptive airfoil is profile planning. The control system is responsible for adapting the wing shape for any given flight condition, such as maximizing the lift/drag ratio. A simple control system can be utilized in much the same manner as controlling conventional ailerons: slight alterations in the airfoil profile (camber) give feedback through changes in motion. A truly adaptive system requires a more complex control system, however. Ideally, the airfoil profile can be arbitrarily chosen based upon current flight conditions. The profile can be determined from a pre-chosen map based solely upon known flight conditions or a more complex system can measure and/or calculate the pressure distribution on the current airfoil and optimize the shape real-time (figure 3).

TEST BED Piezoelectric Arc Airfoil

The guiding philosophy of adaptive wing design is to find the most cost-efficient system using current or nearly available technology. Several guidelines must be considered when designing

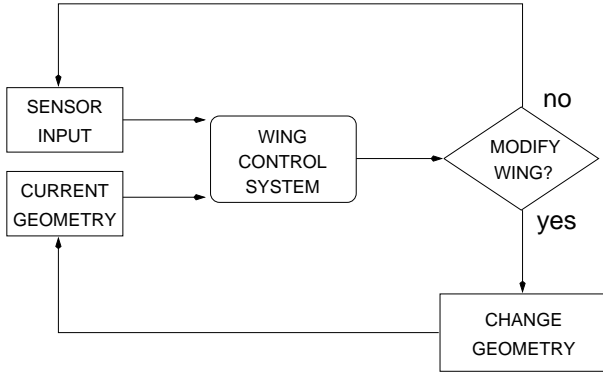


Figure 3. Control functional block diagram.

Control FBD at its simplest level. The purpose of the wing control system is to determine if and what changes should be made from readings of normal aircraft sensor input. This requires extensive training of the wing system with an associated profile database.

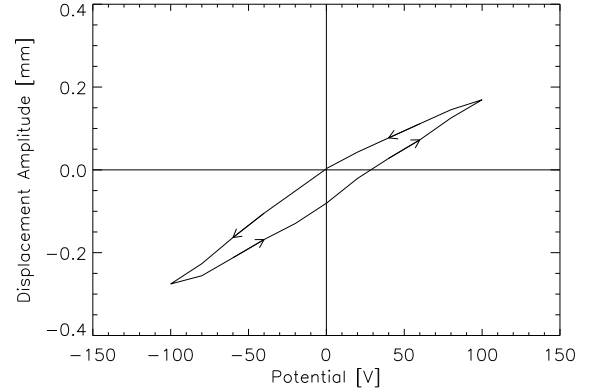


Figure 4. Leading edge displacement.

Displacement of the leading edge versus voltage potential.

this subsystem. These include cost, weight, frequency response, force/deflection, and ease of control. Piezoelectric actuators offer a good balance between these systems. They also lend themselves well to novel applications. Such a design is shown in figure 2. Such a device is currently under development for use in helicopter blades (18). A piezoelectric material is bonded to a substrate. When a voltage is applied to the smart material, the actuator deflects. This deflection is easily controlled by the input voltage. In addition, this system can also be used as a sensor by measuring the output voltage for a given force/deflection input. Thus, this technology can be typically serve dual functions.

The lift for a circular arc airfoil at zero angle of attack can be determined from potential flow theory and is given by

$$L = 4\pi R_c \rho U^2 \sin^2(\phi/4) \quad (1)$$

where R_c is the radius of curvature and ϕ is the subtended arc angle. This can be written in terms of chord-length c as

$$L \approx \frac{\pi}{4} R_c \rho U^2 (c/R_c)^2 \quad (2)$$

or using the definition for section lift coefficient,

$$C_l = \frac{L}{\frac{1}{2} \rho U^2 c} \quad (3)$$

this can be written as

$$C_l = \frac{\pi c}{2R_c} \quad (4)$$

Thus, as $R_c \rightarrow \infty$, $C_l \rightarrow 0$, or the flat plate solution.

A piezoceramic actuator serves as the adaptive airfoil. It is a modified THUNDER (thin-layer composite-unimorph ferroelectric driver and sensor) actuator with $c = 9.7$ cm and $b/2 = 7.1$ cm. It has a thickness of .064 cm (0.025 in.). The typical displacement is approximately 1 cm at maximum allowable input voltage. The baseline (zero potential) radius of curvature R_c of the airfoil is 16 cm. R_c is varied by changing the voltage applied across the arc airfoil. The maximum input voltage varies $R_c \pm 2\%$ resulting in a change in lift coefficient C_l of approximately 7%. R_c can be varied at a frequency f up to 20 kHz. Maximum ΔR_c occurs in the range $f < 25$ Hz. Figure 4 shows the variation in leading edge displacement over a range of ± 100 V. A slight hysteresis is evident.

The displacement and force from a piezoelectric cantilever beam of length c with a dielectric permittivity matrix e_{ij} and applied electric field E can be estimated as follows (20). The differential force, dF , along the beam is given by

$$dF = be_{31} E dy \quad (5)$$

where b is the width of the beam. The differential moment, dM , then is simply

$$dM = be_{31} E y dy \quad (6)$$

This becomes

$$M = e_{31} E \frac{bh^2}{4} \quad (7)$$

where h is the beam thickness. For a cantilever beam, the moment is also given by

$$M = YI \frac{\partial^2 \zeta}{\partial x^2} \quad (8)$$

where Y is the Young's modulus of the material, I is the area moment of inertia, and ζ is the beam displacement. This then gives

$$\frac{\partial^2 \zeta}{\partial x^2} = \frac{3e_{31}E}{Yh} \quad (9)$$

Using boundary conditions

$$\zeta(0) = 0 \quad \frac{\partial \zeta(0)}{\partial x} = 0$$

the maximum displacement, at $x = c$, is found to be

$$\zeta_{max} = \frac{3}{2} (c/h)^2 (e_{31}/Y) V \quad (10)$$

where V is the applied voltage. The equivalent force is then shown to be

$$F = \frac{3\zeta_{max} Y I}{c^3} \quad (11)$$

This result can be used to compare the piezoelectric forces with the aerodynamic forces.

Experimental Facility

The experiments are conducted in a subsonic wind tunnel using two piezoelectric adaptive airfoils as shown in figure 5. Two identical piezoelectric arc airfoils with a chord $c = 9.7$ cm and semi-span $b/2 = 7.1$ cm are available and can be used together or alone. The baseline (zero potential) radius of curvature is $R_c = 16$ cm. The airfoils are mounted on two separate splitter plates and are separated by a distance of $\delta = 5.1$ cm. The airfoils are mounted on the splitter plates at the trailing edge. Thus, an applied voltage changes both the radius of curvature R_c and angle of attack α . The airfoils are powered by a bi-polar operational power supply with a maximum output voltage of 100 V. A function generator is also used to provide sinusoidal input to provide in-phase and out-of-phase oscillations of the piezoelectric arc airfoils. The maximum input frequency for the current experiments is $f = 10$ Hz. A Keyence LK-503 laser displacement sensor is used to measure the displacement of the leading edge.

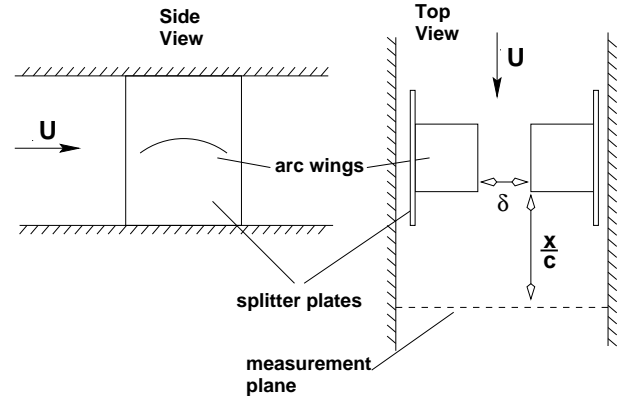


Figure 5. Wind tunnel setup.

Two test wings placed in the wind tunnel for vortex control tests.

The wind tunnel has a test section 152 cm long, 41 cm wide, and 20 cm high. A seven-hole probe Aeroprobe data acquisition system is used to obtain the steady state (time-averaged) experimental data. The system consists of a seven-hole pressure probe, which is connected to an 8 port multi-channel pressure scanner. The probe is mounted on a two-axis traverse, which is connected to two stepping motors and controlled by a multi-axis stepping motor controller. The multi-channel pressure scanner and the multi-axis motor controller are interfaced with a personal computer by a CIO-DAS08 Analog/Digital Board and the ESPIO signal conditioner. All data acquisition parameters and setup are controlled via software. Ensemble averaging is employed. Measurements are made in the cross-stream plane of the wind tunnel (y - z plane) at various downstream locations between $3.1 < x/c < 11.2$ (x -direction) of the trailing edge of the piezoelectric adaptive airfoils. Windows of 0.1×0.04 m and 0.1×0.06 m depending on the downstream location are used for the measurements with a grid spacing of 0.4 cm.

Estimates of the piezoelectric force F and aerodynamic force L show that

$$F \gg L$$

or the deflection of the airfoil due to electric excitation is much larger than the deflection of the airfoil due to aerodynamic forces. This is verified by using the piezoelectric actuator in the sensor mode and measuring the measured output voltage to the input displacement. The displacement is negligible, though the effects of unsteady aerodynamic have not been determined.

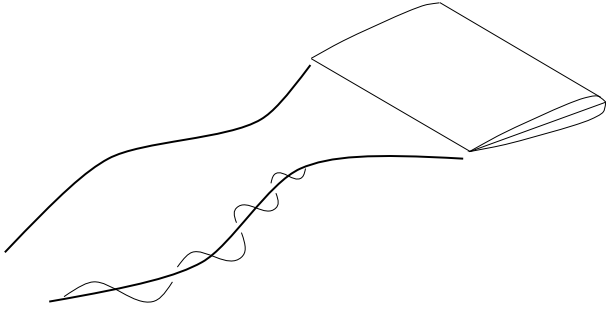


Figure 6. Wing wake instabilities.

Formation of long and short wave instabilities on the vortices within a vortex wake.

PRELIMINARY RESULTS

Wake Vortex Control

This section discusses a possible means of altering the behavior of the vortex wake from airfoils by modifying the vortices with alterations in the airfoil lift. The motivation comes from concerns of controllability of a trailing aircraft in a vortex wake and the persistence of the signature of a lifting body. Loss of controllability, for example, poses a safety hazard on trailing aircraft. Our interest here is driven by air travel safety and, to some degree, by passenger comfort. An unexpected encounter with the wake vortices of a large aircraft is a rather unpleasant event even if the aircrafts are separated by farther than the required distance. We are exploring a possible way of mitigating the potential danger by manipulating the vortices in the wake. Various methods of vortex control and alleviation have been proposed and tested. These include control surface oscillations, wingtip devices, multi-wake interactions, thermal forcing, and mass/momentum injection (e.g., see (21; 22; 23)). It appears that at the time of this writing, no effective method of trailing vortex mitigation has been successfully implemented.

A total of 12 runs of velocity data at several downstream locations were recorded. Velocity of the wind tunnel was kept constant at 10 m/s and a Re based on chord length of $6.6 \cdot 10^5$. The piezoelectric airfoil was subjected to four different voltage potential conditions; baseline (zero voltage), maximum (+100 V), minimum (-100 V), and 10 Hz oscillating (± 100 V sinusoidal). Data were recorded at three different downstream locations, x -axis, at $x/c = 3.2$, $x/c = 6.4$, and $x/c = 11.2$ for each condition. A square data acquisition window size of $40 \text{ mm} \times 40 \text{ mm}$ was used and a total of 121 data points were created to collect data with a grid spacing of 4 mm.

The vortex core growth rate for four different cases are shown in figure 7 for a solitary vortex. The growth rate of the viscous vortex core agrees very well with the prediction by Moore and Saffman, given by the solid line and in general behaves much as described by Batchelor. According to Zeman, the vortex core

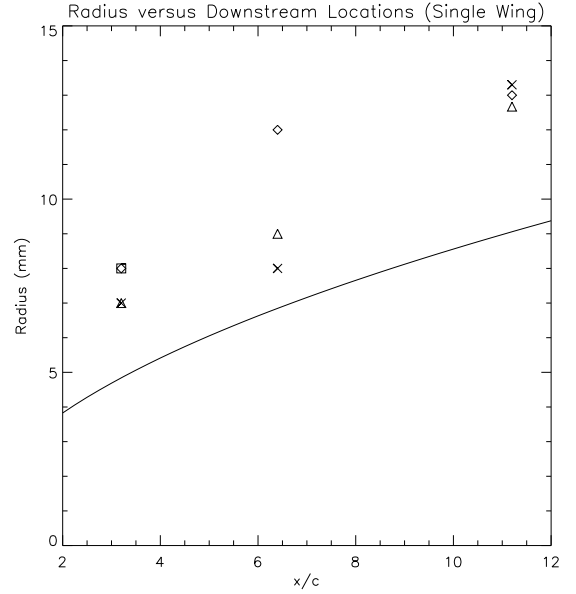


Figure 7. Growth of vortex core radius versus Re_c .

The symbols denote the voltage potential conditions on the wing: $\diamond = \text{Baseline}$, $\triangle = \text{Max}$, $\square = \text{Min}$, $\times = 10\text{Hz}$. Solid line is the theoretical derivation given by Moore and Saffman (1973), $2.92(\Gamma_o/v)^{-1/2}$.

growth rate parameter is defined as

$$\sigma = \frac{\Delta r}{\Delta(\Gamma_o t)^2} = \frac{\Delta r^*}{\Delta z^2} \Gamma_o^{-1/2} \quad (12)$$

where r^* is the dimensionless radius based on chord length, z is the downstream location, and Γ_o is the reference circulation. Figure 8 shows the growth for the vortices from two wings. One wing is specified as the control wing while the other is fixed in the baseline mode for all runs. In figure 8, the former is the lower group of points while the latter is the upper group. For the baseline vortex, the growth rates are unchanged from the case of a single wing. While the growth rate of the fixed vortex is unaffected by the control vortex when the control wing is fixed, the vortex shows a marked decline in growth rate if the control wing has an oscillatory motion. Interestingly, the vortex from the oscillating wing has a growth rate very similar to that if the wing were not oscillating. However, the vortex from the oscillating wing does have an effect on the neighboring vortex and effectively slows the growth rate of that vortex. This indicates that by altering the nature of a control vortex, one can modify the behavior of an unrelated vortex.

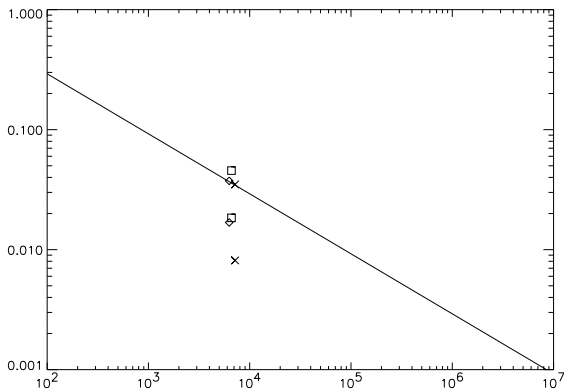


Figure 8. Vortex wake growth rates.

Symbols defined as in figure 8. Growth rate of the vortex cores. Solid line is the theoretical derivation given by Moore and Saffman (1973), $2.92(\Gamma_o/v)^{-1/2}$. The growth rate for four different cases agree very much with Moore and Saffman. The non-oscillating vortex growth rate is slowed by the oscillating vortex whose growth rate is unaffected.

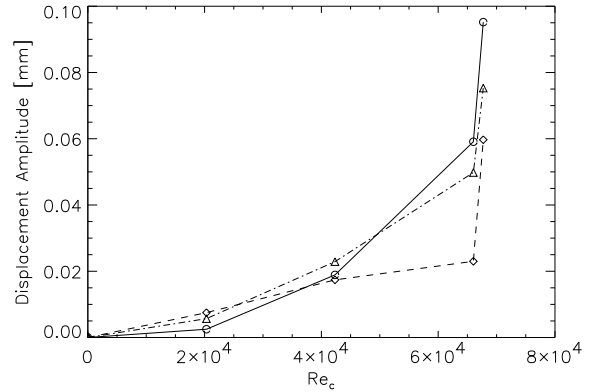


Figure 9. Leading edge displacement versus Re_c .

○ baseline (0 V), ◇ maximum (+100 V), △ (-100 V).

Flutter Control

Control of flutter is of great importance in many aerodynamic applications, from control surfaces on aircraft to airfoil cascades in turbine engines. Active flow control has played a large part in flutter research in recent years, but has focused on flutter control by using blowing and/or suction or MEMS devices. Both of these concepts attempt to essentially alter the boundary layer on the surface which may in turn alter the flow conditions causing flutter. In other words, the devices alter the flow to adapt to the surface. With a shape adaptive wing, the opposite approach is used; the surface adapts to changing flow conditions.

Figure 9 shows results of flutter tests on a single wing placed in the wind tunnel. The leading edge displacement is shown as a function of Reynolds number for 3 different cases: baseline, maximum, and minimum voltage conditions; frequency was not measured. The flutter amplitude is largest in the baseline case where no voltage potential is applied and the wing is free to vibrate. The displacement amplitude increases dramatically as $Re_c > 6 \cdot 10^4$. For both cases where voltage was applied, the maximum displacement was less than that of the baseline mode except in cases where the flow velocity and displacements were small. Note that the lowest maximum amplitude at high Re_c occurs for +100 V, where Re_c of the airfoil has increased also increasing the angle of attack and the total lift on the wing. This indicates that the lift on the wing is acting to dampen the vibration. In the -100 V case, however, the flutter amplitude is also lowered, but now due to the piezoelectric force on the wing.

ACKNOWLEDGMENT

The authors would like to thank Profs. John Main and H. S. Tzou of the University of Kentucky for their helpful discussions on the fields of structural dynamics and adaptive materials.

REFERENCES

- (1) I. Wygnanski. "On Active Flow Control: A Personal Perspective," 39th Israel Annual Conference on Aerospace Sciences, Tel-Aviv, February, 1999.
- (2) J. D. Jacob. "On the Fluid Dynamics of Adaptive Airfoils," Proc. of the 1998 ASME International Mechanical Engineering Congress and Exposition, Anaheim, CA, 1998.
- (3) P. B. S. Lissaman. "Low-Reynolds-Number Airfoils," *Annual Review of Fluid Mechanics*, **15**, 223-39, 1983.
- (4) T. J. Mueller (ed.). *Low Reynolds Number Aerodynamics*, Springer-Verlag, New York, 1989.
- (5) J. M. McMichael and M. S. Francis., "Micro Air Vehicles - Toward a New Dimension in Flight," DARPA Document, 1997.
- (6) T. A. Weisshaar. "Aeroelastic Tailoring-Creative Use of Unusual Materials," AIAA Paper 87-0976, April 1987.
- (7) S. M. Ehlers and T. A. Weisshaar. "Static Aeroelastic Behavior of an Adaptive Laminated Piezoelectric Composite Wing," AIAA Paper 90-1078-CP.
- (8) J. Austin, J. Rossi, W. Van Nostrand, G. Knowles, and A. Jameson. "Static Shape Control for Adaptive Wings," *AIAA Journal*, V. 32, No. 9 (September 1994), pp. 1895-1901.
- (9) L. Librescu, L. Meirovitch, and O. Song. "Integrated Structural Tailoring and Control Using Adaptive Materials for Advanced Aircraft Wings," *Journal of Aircraft*, Vol. 33, No. 1 (January-February 1996), pp. 203-213.
- (10) J. L. Pinkerton, A. R. McGowan, R. W. Moses, R. C. Scott, and J. Heeg. "Controlled Aeroelastic Response and Air-

foil Shaping Using Adaptive Materials and Integrated Systems,” SPIE Paper 0-8194-2092-1 in SPIE Vol. 2717, pp. 166-177, 1994.

(11) C. L. Hustedde, S. F. McGrath, M. A. Hopkins, and K.E. Griffin. “Further Investigations of the Aeroelastic Tailoring for Smart Structures Concept,” Proceedings of the AIAA 38th Structures and Structural Dynamics Conference, Kissimmee, Florida, April 7-10, 1997, AIAA Paper 97-1164.

(12) J. Kudva, K. Appa, C. A. Martin, A. P. Jardine, G. Sendekyj, T. Harris, A. McGowan, and R. Lake. “Design, Fabrication, and Testing of the DARPA / Wright Lab Smart Wing Wind Tunnel Model,” Proceedings of the AIAA 38th Structures and Structural Dynamics Conference, Kissimmee, Florida, April 7-10, 1997, AIAA Paper 97-1198.

(13) J. L. Pinkerton and R. W. Moses. “A Feasibility Study to Control Airfoil Shape Using THUNDER,” NASA TM-4767, November, 1997.

(14) M. S. Chandrasekhaara, M. C. Wilder, and L. W. Carr. “Design and development of a Dynamically Deforming Leading Edge Airfoil for Unsteady Flow Control,” *ICIASF '97*, 1997.

(15) S.-H. Kim and I. Lee. “Aeroelastic Analysis of a Flexible Airfoil with a Freeplay Non-linearity,” *Journal of Sound and Vibration*, 193(4):823-846, 1996.

(16) W. Shyy and R. Smith. “A Study of Flexible Airfoil Aerodynamics with Application to Micro Aerial Vehicles,” AIAA 97-1933, *28th AIAA Fluid Dynamics Conference*, June, 1997.

(17) F. K. Straub and D. J. Merkley. “Design of a Smart Material Actuator for Rotor Control,” *Smart Materials and Structures*, 6:26-34, 1997.

(18) J. W. Clement, D. Brei, D., A. J. Moskalik, and R. Barrett. “Bench-top Characterization of an Active Rotor Blade Flap System Incorporating C-Block Actuators,” 39th AIAA/ASME/ASCE/AHS/ASC Structures, Structural Dynamics, and Materials Conference and Exhibit, AIAA-98-2108, 1998.

(19) O. K. Rediniotis, D. C. Lagoudas, L. J. Garner, and N. Wilson. “Experiments and Analysis of an Active Hydrofoil with SMA Actuators,” AIAA 36th Aerospace Sciences Meeting and Exhibit, AIAA-98-0102, 1998.

(20) H. S. Tzou. “Development of a Light-Weight Robot End-Effector Using Polymeric Piezoelectric Bimorph,” *Proc. of the 1989 IEEE International Conference on Robotics and Automation*, Scottsdale, AZ, 1989.

(21) J. H. Olsen, A. Goldberg, and M. Rogers, editors. *Aircraft Wake Turbulence and its Detection*. Plenum Press, 1971.

(22) A. Gessow, editor. *Symposium on Wake Vortex Minimization*. NASA, 1976. NASA SP-4096.

(23) J. N. Hallock. “Aircraft Wake Vortices: An assessment of the current situation.” Technical Report DOT-FAA-RD-90-20, DOT-VNTSC-FAA-90-6, U.S. Department of Transportation, John A. Volpe National Transportation Systems Center, Cambridge, MA, 1991.

(24) D. W. Moore and P. G. Saffman. “Axial Flow in Laminar

Trailing Vortices,” *Proceedings of the Royal Society of London A*, 333:491-508, 1973.

(25) G. K. Batchelor. “Axial Flow in Trailing Line Vortices,” *Journal of Fluid Mechanics*, 20:645-658, 1964.

(26) O. Zeman. “The Persistence of Trailing Vortices,” *Physics of Fluids*, 71(1) :135-143, 1995.